Potential barriers in the migration of tracer oxygen atoms in the $YBa_2Cu_3O_{7-\delta}$ lattice

V. B. Vykhodets, T. E. Kurennykh, K. V. Trifonov, A. Ya. Fishman, and A. A. Fotiev

Institute of Physics of Metals, Ural Branch of the Russian Academy of Sciences, 620219 Ekaterinburg, Russia
(Submitted 6 April 1994)
Zh. Eksp. Teor. Fiz. **106**, 648–662 (August 1994)

We conducted experimental and theoretical investigations of the diffusion of tracer oxygen atoms in $YBa_2Cu_3O_{7-\delta}$ in isochronous and isothermal annealing. We demonstrate that in specially selected conditions of annealing samples in gaseous oxygen enriched with the ^{18}O isotope, ^{18}O atoms are consecutively substituted for ^{16}O atoms in the positions and planes of different types in the oxygen sublattice of the compound. The observed position-planar effect is used to extract information about the diffusion mechanism and to determine the heights of the energy barriers, which characterize the isotopic exchange inside the crystal and at the gas–solid interface. By means of this technique we obtain a much fuller set of diffusion parameters than is done in conventional approaches. We show that high-T_c superconducting oxides with a quasiplanar structure and an anomalously high anisotropy of the diffusion properties must be distinguished as a special class of diffusion systems for which the phenomenological Fick equations are inadequate to describe the diffusion of oxygen in ordinary temperature–temporal annealing conditions. We suggest an alternative approach to describe diffusion in such systems.

1. INTRODUCTION

For high-T_c superconducting oxides with a quasiplanar structure the information about the diffusion processes and defects in the oxygen subsystem obtained from diffusion measurements is quite limited. With conventional methods it is impossible to derive from the experimental data a complete set of values of the heights of the energy barriers and the hopping rates, which characterize the migration of oxygen atoms. For instance, when there is diffusion in a $YBa_2Cu_3O_{7-\delta}$ crystal in the direction of the z axis, the following oxygen-atom hopping sequence is possible between positions: O1 or O5 (the $CuO_{1-\delta}$ plane) → O4 (BaO) → O2 or O3 (CuO_2) → O2 or O3 (CuO_2) → O4 (BaO) → O1 or O5 ($CuO_{1-\delta}$). Here, in reality, the temperature dependence of the diffusion coefficient D_{zz} yields only the value of the activation energy that characterizes the highest energy barrier in the diffusion along the z axis. The absence of data on the heights of the other potential barriers makes it impossible to identify in a unique manner the diffusion mechanism and the type of defects responsible for the migration of atoms.

In this paper we suggest an alternative way of studying the diffusion of tracer oxygen atoms in high-T_c superconductors with a quasiplanar structure. The underlying method is that of isochronous sample annealing. This approach has found the widest acceptance in studying the behavior of nonequilibrium point defects in solids[1] where defects of several types are present. Often the researcher is able to select experimental conditions such that practically complete annealing of defects of each type is localized in a narrow temperature range. This enables one to identify several elementary stages in the complex process and the characteristics of each stage, e.g., the activation energy. In experiments of this kind the kinetics manifests itself in the appearance of several peaks on the curve representing the temperature (T) dependence of $\partial c/\partial T$, where c is the defect concentration in the sample, and T is the sample temperature.

We used the isochronous annealing method to study the isotopic exchange in oxygen between the high-T_c superconducting crystal and the gas phase enriched with the ^{18}O isotope. The existence of several types of equilibrium positions for the oxygen atoms in such crystals suggests that the kinetics of substitution of ^{18}O atoms for ^{16}O atoms is similar to that observed in the annealing of nonequilibrium point defects in solids. Here three types of substitution effects are possible: position, planar, and position–planar. Position effects are characterized by consecutive substitution of the equilibrium positions of each type in the lattice. For such kinetics the number of isochronous annealing peaks on the $\partial c/\partial T$ vs T curve (c is the concentration of the ^{18}O isotope in the sample) and the number of equilibrium-position types in the high-T_c superconducting crystal must coincide. In the case of planar effects the ^{18}O atoms consecutively occupy certain crystallographic planes. Position–planar effects correspond to mixed kinetics.

Multiple isochronous annealing peaks can be observed during isotopic exchange only if the activation energies of the various processes differ considerably. In this sense high-T_c superconducting compounds with a quasiplanar structure are unique objects with a record-breaking anisotropy of diffusion coefficients and a marked difference in the activation energies for the $\mathscr{D}_{zz}$ and $\mathscr{D}_{xx}$. In yttrium and bismuth high-T_c superconductors the $\mathscr{D}_{xx}/\mathscr{D}_{zz}$ ratios are 10^5–10^6 for tracer oxygen atoms, and the diffusion activation energies in the basal planes and along the z axis differ more than by 1 eV (see Refs. 2–5).

The experimental setting and the data processing method were based on a meaningful microscopic model of the phenomenon. The choice of features of the model depended on the specifics of the diffusion processes in the system, which

 1063-7761/94/080355-09$10.00 © 1994 American Institute of Physics

was characterized by highly anisotropic diffusion coefficients and the presence of several equilibrium-position types.

2. THE EXPERIMENT

2.1. Samples

In our experiment we used an yttrium superconductor with 123 composition. In choosing the parameters of the sample we allowed for the fact that the kinetics of the diffusion processes depends sensitively on the relation between the sample linear dimensions b and the characteristic diffusion parameter $\sqrt{\mathscr{D}\tau}$. The conditions for distinguishing the isochronous annealing peaks are most favorable for $b<\sqrt{\mathscr{D}\tau}$, that is, when the filling of one subsystem of the oxygen sublattice can be completed in the initial annealing stage. For this reason a finely dispersed powder proved to be the best type of sample for our studies. Our method, however, enables the concentration of oxygen isotopes to be measured only in massive samples. Allowing for these contradictory requirements we used samples prepared by powder caking, which, however, had a density of 70% of the theoretical value. Special experiments have shown that the isotopic exchange kinetics in such objects proves be essentially the same for crystallites outcropping from the outer surface and for those several tens of micrometers below the surface, that is, gaseous oxygen easily penetrates the space between grains in the annealing process. For such samples it is relatively easy to select a regime of isochronous annealing that ensures this condition $b\leqslant\sqrt{\mathscr{D}\tau}$ already in the initial stage of the experiment.

Radiographic studies show that the $YBa_2Cu_3O_{7-\delta}$ ceramics under investigation exists only in one phase. The average size of the crystallites was several micrometers. The temperature and width of the superconducting transition proved to be 90 K and 1.0 K, respectively.

Diffusion annealing was conducted in a quartz tube in an oxygen environment 80%-enriched with the ^{18}O isotope maintained at a pressure of 1 atm. The isotopic composition of the gaseous phase was monitored in special experiments and was shown to remain constant during annealing. The isobaric conditions of the experiment are not, of course, optimal and are due to the high cost of ^{18}O. In view of this, in interpreting the results we allow for the decrease in the total number of oxygen atoms in the samples as the annealing temperature is raised.[6] For the temperature interval used in the experiment this variation amounted to several percentage points. The isobaric annealing regime may also cause nonrandom oxygen atom migration and a related change in the migration rate. The data from Ref. 2 suggest that this effect is unimportant; in similar experimental conditions no anomalies in the $YBa_2Cu_3O_{7-\delta}$ ceramic were observed that would corroborate the idea that the driving forces have a noticeable effect on the diffusion coefficients of the tracer oxygen atoms.

The isothermal exposure in the isochronous annealing lasted four hours, and the temperature of each subsequent annealing exceeded that of the previous by 20 °C. In addition to isochronous annealing we also performed isothermal annealing. The combination of the two regimes was used to determine the activation energy in each stage of annealing.[1] It took less than 10 min to reach a constant temperature. After each annealing the sample was cooled to room temperature and the concentration of oxygen isotopes was measured. The cooling time was approximately 1 min. The temperature was measured by a Chromel–Alumel thermocouple with an accuracy of ±1 °C. During annealing the quartz tube was placed inside a massive metal cylinder. In view of this, to within the specified accuracy of the measurements, no temperature gradients were observed where the sample was.

2.2. Measurements of concentration profiles

The concentration profiles of the ^{18}O isotope were measured nondestructively down to a depth of one micrometer by the nuclear microanalysis method. The reaction used here was $^{16}O(p,\alpha)^{15}N$ with a primary-beam particle energy of 762 keV. The diameter of the primary proton beam was 1 mm, that is, concentration measurements were done with averaging over a large number of crystallites. The plane of the samples being studied was positioned perpendicular to the primary-beam axis, and the angle at which the nuclear reaction products were detected was equal to 160°. The energy spectrum of the alpha particles was measured by a silicon surface-barrier detector about 10 mm in diameter. The root-mean-square error was less than 10% in the measurements of the lowest concentrations of the ^{18}O isotope and 3% in measurements of high concentrations. Basically, we could have achieved greater accuracy, but we preferred a lower dose of radiation of the samples. We also measured the concentration of the ^{16}O isotope so as to monitor the initial samples and those that had undergone a complete cycle of isochronous annealing. The reaction used in this case was $^{16}O(d,p_1)^{17}O^*$ with a primary-beam particle energy of 900 keV. The statistical error in determining the concentrations amounted to 1%. The other experimental conditions for irradiating the samples with deuterons were the same as in the $^{16}O(p,\alpha)^{15}N$ reaction. We found that down to a depth of about 1 μm the overall concentration of oxygen isotopes in the samples decreased by a factor of 1.06 ± 0.03 as a result of isochronous annealing in the 320–670 °C temperature range. This value does not contradict the variation in the deficit δ in oxygen in $YBa_2Cu_3O_{7-\delta}$ samples expected in annealing.[6]

2.3. Results

The data depicted in Fig. 1 characterize the variation in the concentration of the ^{18}O oxygen in samples that had undergone isochronous annealing as a function of the temperature maintained in the experiment (see also Ref. 7). These results correspond to a depth of 0.15 μm in the sample. The specific values play no important role since under the experimental conditions there was practically no gradient in the concentration of ^{18}O. Only at the lowest temperatures and shortest annealing times was the difference in the concentrations of ^{18}O at the surface and at a depth of 1 μm considerable, amounting to about 25%.

Four peaks of isochronous annealing are clearly visible in Fig. 1. The characteristics of the peaks are listed in Table

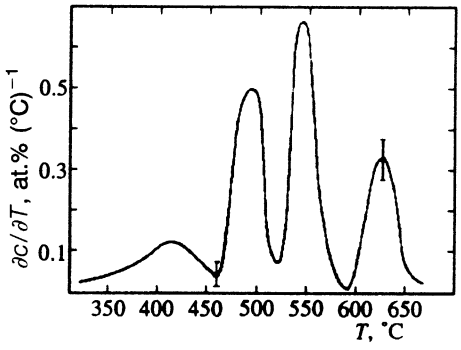

FIG. 1. Isochronous annealing peaks.

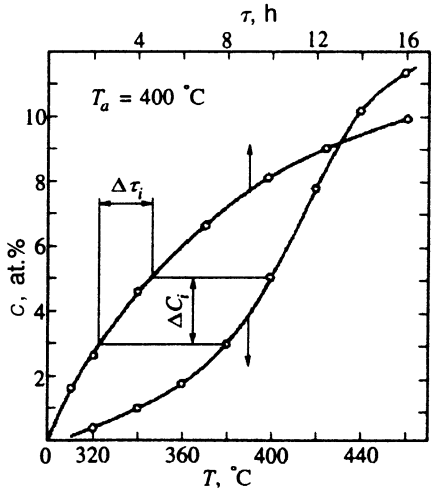

FIG. 2. The isotherm $c(\tau)$ and the isochrone $c(T)$ for the first stage of annealing.

I, where the T_n are the temperatures corresponding to the maximum values of the function $\partial c/\partial T$, c_n is the concentration of the ^{18}O isotope at the moment when the peak has completely formed, $\Delta c_n/\gamma$ is the increase in the ^{18}O isotope concentration at the given annealing peak, and $\gamma=0.8$ is the degree of enrichment of oxygen with the ^{18}O isotope. The values of $\Delta c_n/\gamma$ correspond to hypothetical conditions in which the gaseous phase contains only atoms of the ^{18}O isotope. The normalization conditions for the concentration were chosen so that a value of 100% corresponds to the filling of all the positions in the oxygen sublattice of the compound.

The peaks were identified by comparing the concentrations x_n of the oxygen atoms at different positions of the $YBa_2Cu_3O_{7-\delta}$ lattice (see Table I) and the values of $\Delta c_n/\gamma$. Clearly, the first peak corresponds to ^{18}O atoms being substituted for ^{16}o atoms in the positions in the $CuO_{1-\delta}$ plane. The experiment revealed no fine structure in the peak; such a structure could exist if this plane had two types of positions, O1 and O5.

The value $\Delta c_2/\gamma$ is close to x_n for positions O4 in the BaO plane and for positions O2 and O3 in the CuO_2 plane. Since position O4 is geometrically closer to the $CuO_{1-\delta}$ plane, it can be assumed that in the second annealing stage the ^{18}O atoms are substituted for ^{16}O atoms in the positions in the BaO plane.

The results for the values of $\Delta c_n/\gamma$ for the third and fourth peaks proved somewhat unexpected: $\Delta c_3/\gamma > c_4/\gamma$ and $\Delta c_3/\gamma > x_3$. Since in the tetragonal phase of the $YBa_2Cu_3O_{7-\delta}$ compound the positions O2 and O3 are indistinguishable, the above inequalities emerge because of an ortho–tetra phase transition. The reasons for the transition of several percentage points of the orthorhombic phase to the tetragonal at such low temperatures may be the concentration inhomogeneities in the cation sublattice of the compound or multiple proton irradiation of the samples. There are no sufficient grounds for identifying the third and fourth peaks reliably. Most likely, the third peak corresponds to the substitution of ^{18}O atoms for ^{16}O atoms in positions O3, since the lattice parameter for the tetragonal phase in the basal plane is closer to the lattice constant along the y axis in the orthorhombic. The total concentration variation $\Sigma_{n=1}{}^4\Delta c_n/\gamma$ amounted to 92.5%. This considerable deficit in oxygen is apparently due to the isobaric conditions of the experiment, that is, in annealing not only ^{18}O atoms were substituted for ^{16}O atoms but also the number of oxygen atoms in the sample decreased.

Figures 2–5 depict two types of curves representing the temperature and temporal dependence of the concentration of the ^{18}O isotope: isochrones $c(T)$ and isotherms $c(\tau)$. The isotherms $c(\tau)$ are obtained for certain characteristic values of temperature T_a for each of the four peaks (the values of T_a are given in the figures). The data on $c(\tau)$ and $c(T)$ correspond to a depth of 0.15 μm in the samples. The samples for isothermal annealing at $n=2,3,4$ were prepared in a special way: in each case isochronous annealing was done prior to isothermal, which ensured that isotopic exchange was finalized in the previous stages. For instance, before $c(\tau)$ was measured at 630 °C, the sample was annealed isochronously, and this formed the peaks with $n=1,2,3$.

There are several methods for determining the activation

TABLE I. Characteristics of isochronous annealing peaks.

No. of peak	T_n °C	c_n at.%	$\Delta c_n/\gamma$	x_n	Occupied positions	E_n eV	ν_n s^{-1}
1	415	11.4	14.2	$14.28(1-\delta)$	O1 and O5	1.08±0.04	–
2	495	33.7	27.9	28.56	O4	1.65±0.15	4.4×10^6
3	545	61.0	34.1	28.56	O3	2.26±0.04	4.7×10^9
4	626	74.0	16.3	28.56	O2	2.93±0.02	1.5×10^{12}

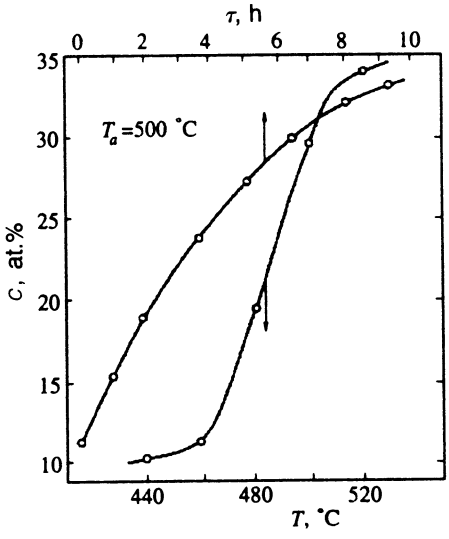

FIG. 3. The isotherm $c(\tau)$ and the isochrone $c(T)$ for the second stage of annealing.

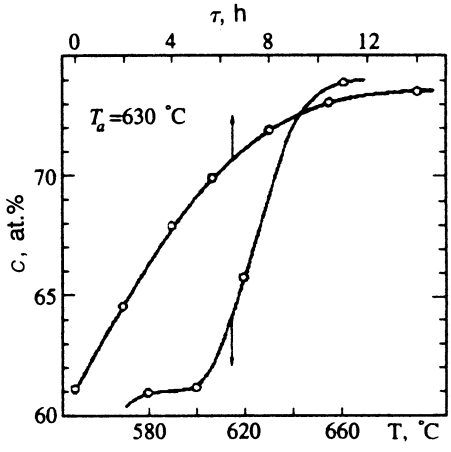

FIG. 5. The isotherm $c(\tau)$ and the isochrone $c(T)$ for the fourth stage of annealing.

energies of processes responsible for the formation of isochronous annealing peaks for point defects.[1] The method we employed is based on processing the data of combined isothermal and isochronous annealing. The result obtained by this method should be accepted with caution because the kinetics of isotopic exchange includes the transfer of oxygen atoms across the gas–solid interface.

This method of determining the activation energy presupposes calculation of the temperature dependence of a certain characteristic time interval $\Delta\tau$ from the known $c(\tau)$ and $c(T)$ curves. An example of calculating one such value $\Delta\tau_i$ is illustrated by Fig. 2, where Δc_i stands for the variation of the concentration of the ^{18}O isotope in the sample in the ith isothermal exposure during isochronous annealing. If the annealing stage is characterized by only one value of the activation energy, the $\ln(\Delta\tau)$ vs $1/T$ dependence (T is measured in K) must be represented by a straight line whose slope gives the activation energy of the process.[1] The corresponding experimental data are depicted in Fig. 6. The numbers at the lines designate the number of the annealing peak. Clearly, $\delta\tau$ obeys an exponential dependence satisfactorily. The activation energy values are listed in Table I.

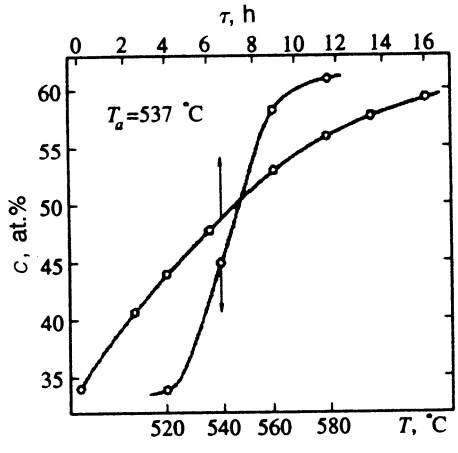

FIG. 4. The isotherm $c(\tau)$ and the isochrone $c(T)$ for the third stage of annealing.

3. THEORY

3.1. A model of isotopic exchange in $YBa_2Cu_3O_{7-\delta}$

The main laws governing isotopic exchange are analyzed using the example of a single-crystal sample. Generalization to the case of a polycrystalline sample presents no real difficulties.

Suppose that initially the oxygen subsystem of the $YBa_2Cu_3O_{7-\delta}$ crystal contains only ^{16}O atoms and that the sample is placed in an atmosphere of ^{18}O maintained at constant temperature and pressure. We assume that there are no concentration gradients in the oxygen isotopes in the y and z directions and that the composition of the gaseous atmosphere and the total number of oxygen atoms in the crystal do not change in the course of annealing.

Let us imagine the $YBa_2Cu_3O_7$ as a stack of identical layers, each of which contains the following set of planes: $Y–CuO_2–BaO–CuO_{1-\delta}–BaO–CuO_2–Y$. We denote the concentration of the ^{18}O atoms in the ith plane at time τ at a distance x from the surface by $C^{(i)}\equiv C^{(i)}(x,\tau)$, the fraction of positions in the layer's ith plane unoccupied by oxygen by V_i, and the probability of an oxygen atom hopping from a position in the ith plane to the closest positions in the jth plane by P_{ij}. Then the temporal variation of the concentrations $C^{(i)}$ is described by the following system of partial differential equations:[8]

$$\frac{\partial C^{(1)}}{\partial t}=-\frac{2\mu}{1-\delta}C^{(1)}+\mu C^{(2)}+D_{xx}^{(1)}\frac{\partial^2 C^{(1)}}{\partial x^2},$$

$$\frac{\partial C^{(2)}}{\partial t}=\frac{2\mu}{1-\delta}C^{(1)}-(\mu+2\kappa)C^{(2)}+\kappa C^{(3)}+D_{xx}^{(2)}\frac{\partial^2 C^{(2)}}{\partial x^2},$$

$$\frac{\partial C^{(3)}}{\partial t}=2\kappa C^{(2)}-\kappa C^{(3)}+D_{xx}^{(3)}\frac{\partial^2 C^{(3)}}{\partial x^2},\quad t\equiv\frac{\tau P_{11}V_1}{\tau_0},\qquad(1)$$

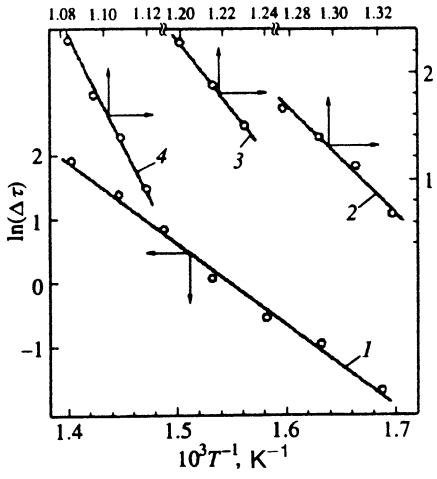

FIG. 6. Curves representing the temperature dependence of the time $\Delta\tau$ for different annealing stages ($n=1,2,3,4$).

$$\mu=\frac{P_{21}}{P_{11}}, \quad \kappa=\frac{P_{32}V_2}{P_{11}V_1},$$

$$P_{12}V_2\simeq 2P_{21}V_1, \quad P_{23}V_3\simeq 2P_{32}V_2,$$

$$D_{xx}^{(2)}=1, \quad D_{xx}^{(2)}=\frac{P_{22}V_2}{P_{11}V_1}, \quad D_{xx}^{(3)}=\frac{P_{33}V_3}{P_{11}V_1}.$$

Here we have postulated that an elementary hopping act requires that there be a vacancy in the final position, and we have allowed only for the hopping of oxygen atoms between the closest positions in the same plane or neighboring planes; τ_0 and a are the hopping time and length for oxygen in the $CuO_{1-\delta}$, and t and x are the dimensionless time and position ($x=x/a$). For simplicity, in the system of equations (1) we ignore the differences between the two types of sites in the orthorhombic phase both in the $CuO_{1-\delta}$ plane and in the CuO_2 plane. If necessary, the system (1) can be augmented by additional equations, and we can also allow for the fact that the occupation by ^{18}o atoms of positions O2 and O3 is related to different activation energies.

Clearly, in the absence of oxygen exchange between planes, that is, $\mu=\kappa=0$, the system of equations (1) splits into three independent equations of ordinary one-dimensional diffusion with coefficients $\mathscr{D}_{xx}^{(i)}$. These are related to the $\mathscr{D}_{xx}^{(i)}$ that act as diffusion parameters in the space of the dimensionless variables x and t through the following relations:

$$D_{xx}^{(i)}=\mathscr{D}_{xx}^{(i)}\frac{\tau_0}{P_{11}V_1a^2}.$$

On the other hand, if we ignore the transport processes in the BaO and CuO_2 planes, that is, if we assume that $D_{xx}^{(2)}=D_{xx}^{(3)}=0$, the system of equations (1) becomes similar to the Fisher equations, which describe diffusion processes in polycrystals (see, e.g. Ref. 9). Here the accelerated diffusion of oxygen in the single crystal occurs in the $CuO_{1-\delta}$ planes, and the slow drain of the ^{18}O isotope from these planes is determined by the exchange of oxygen between $CuO_{1-\delta}$ and BaO planes and between BaO and CuO_2 planes.

The analysis of Eqs. (1) in Ref. 8 has shown that the nature of the solutions depends sensitively on the diffusion annealing time. Over a broad time interval, determined by consecutive switch-on of the different drain mechanisms, the continuous-medium approximation for diffusion may not work. The expressions obtained in Ref. 8 for the total concentration $C(x,t)=\Sigma_{i=1}^{3}C^{(i)}(x,t)$ of the ^{18}O isotope in the crystal refer, however, to boundary conditions corresponding to an infinite rate of isotope exchange between $CuO_{1-\delta}$ planes and the gaseous phase. The results listed in Sec. 2 show that the constant-source approximation for the system under study is not realized. On the contrary, as Figs. 2–5 indicate, in isothermal annealing there is a constant increase in concentration of the ^{18}O near the sample's surface. The effect on the kinetics of the process of the finite rate of isotopic exchange between the gaseous phase and a $CuO_{1-\delta}$ plane can be taken into account via the following boundary condition:

$$\frac{\partial C^{(1)}(0,t)}{\partial x}=-\frac{2\mu}{1-\delta}C^{(1)}(0,t)+\mu C^{(2)}(0,t)+\frac{\partial C^{(1)}(0,t)}{\partial x}+\eta[1-\delta-C^{(1)}(0,t)], \tag{2}$$

where η is a parameter describing the rate of isotopic exchange in the crystal–gaseous-phase interface. Equation (2) allows for the presence of a potential barrier at the gas–solid interface and takes into account the isotopic

exchange in the $CuO_{1-\delta}$ plane and between $CuO_{1-\delta}$ and BaO planes. The Laplace transform $C(x,p)$ of the solution $C(x,t)$ of the system of equations (1) with boundary conditions (2) is

$$C(x,p)=\frac{\eta(1-\delta)f(p)}{p[pf(p)+\eta+\sqrt{pf(p)}\,]}\exp\{-x\sqrt{pf(p)}\}, \tag{3a}$$

$$C(x,p)=\frac{\eta(1-\delta)[f(p)/p]\cosh[(x-b)\sqrt{pf(p)}\,]}{[pf(p)+\eta]\cosh[b\sqrt{pf(p)}2]+\sqrt{pf(p)}\,\sinh[b\sqrt{pf(p)}2]}, \tag{3b}$$

where (3a) and (3b) correspond to the cases of a semi-infinite sample and a sample whose size is $b \equiv ba$, and

$$f(p)=\frac{p^2+p[\mu(3-\delta)/(1-\delta)+3\kappa]+\mu\kappa(7-\delta)/(1-\delta)}{p^2+p(\mu+3\kappa)+\mu\kappa}.$$

Only in some limiting cases do the expressions for $X(x,t)$ assume such simple analytical forms as Eqs. (3). In view of this we introduced a mathematical model for processes of isotopic exchange in which the diffusion parameters varied within a broad range. The results are listed in Sec. 3.2. In the present section, however, we examine the asymptotic relations determining the main laws governing isotopic exchange. To illustrate the role of the activation barrier at the gas–solid interface, we first ignore the isotopic exchange between the basal planes of the crystal (the drain effects). Then, according to (3a), the concentration of the ^{18}O isotope in a semi-infinite sample is

$$\frac{C(x,t)}{C_0}=\operatorname{erfc}\ y+\frac{\eta\exp\{x\eta_-+t\eta_-^2\}}{\eta_--2\eta}\operatorname{erfc}(y+\eta_-\sqrt{t}\,)$$
$$+\frac{\eta\exp\{x\eta_++t\eta_+^2\}}{\eta_+-2\eta}\operatorname{erfc}(y+\eta_+\sqrt{t}\,), \qquad (4)$$
$$\eta_\pm=\frac{1\pm\sqrt{1-4\eta}}{2},\quad y=\frac{x}{\sqrt{4D_{xx}^{(1)}\tau}}=\frac{x}{2\sqrt{t}},$$

where C_0 is the equilibrium value of concentration at the interface. The most interesting case is with $\eta \ll 1$, when (4) differs from the $C_s(x,t)$ obtained in the constant-source approximation. The ratio $C(x,t)/C_s(x,t)$ proves to be much less than unity and

$$\frac{C(x,t)}{C_s(x,t)}\sim\eta\sqrt{t}$$

if the diffusion annealing times are fairly short: $t \ll R/\eta^2$, where $R=x\eta$ for $x\eta \geqslant 1$ and $R=1$ for $x\eta<1$. At fairly long annealing times, $t \geqslant R/\eta^2$, the concentration $X(x,t)$ asymptotically approaches $C_s(x,t)$. For instance, at $y=x\sqrt{4D_{xx}^{(1)}\tau}>1$ [the tail of the concentration profile $C(x,t)$] we have

$$\frac{C(x,t)}{C_s(x,t)}=\frac{2\eta t}{x(1+2\eta t/x)}+\frac{\eta}{1+2t/x}. \qquad (5)$$

Clearly, for the concentration $C(x,t)$ to reach the value of $C_s(x,t)$ at a depth x the annealing times must be so long that the number of ^{18}O atoms crossing the interface is approximately equal to the number of sites along the diffusion path. The characteristic concentration profiles $C(x,t)$ for a finite rate of isotopic exchange at the interface are depicted in Fig. 7.

Similar effects for a sample whose size along the x axis is b are described, according to Eq. (3b), by the formula

$$C(x,t)=1-\eta b^2\sum_{k=1}^{\infty}\times\frac{\cos[z_k(2x/b-1)]\exp\{-4t(z_k/b)^2\}}{z_k^2(4+b)\cos z_k+(z_k/2)(2b+\eta b^2-z_k^2)\sin z_k}, \qquad (6)$$

where z_k is the kth root of the equation $\eta b^2-4z^2=2bz\tau gz$. When η is small, the first term with $k=1$ in the sum provides the main contribution. For a finite sample the most interesting case is when $\eta b \ll 1$. Then $z_1=\sqrt{\eta b/2}$ and Eq. (6) yields

$$C(x,t)=1-\cos\left[\sqrt{\frac{\eta b}{2}}\left(\frac{2x}{b}-1\right)\right]\exp\left\{-\frac{2\eta t}{b}\right\}$$
$$=1-\exp\left\{-\frac{2\eta t}{b}\right\}+\eta b\left(\frac{x}{b}-\tfrac{1}{2}\right)^2\exp\left\{-\frac{2\eta t}{b}\right\}. \qquad (7)$$

Clearly, the concentration profile exhibits a weak parabolic dependence, and it takes $r \geqslant b/\eta$ for the isotope concentration at the interface to reach the equilibrium value. In these conditions the concentration in grain size evens out faster than it grows at the interface.

Our analysis has shown (see, e.g., Fig. 7) that in the presence of an activation barrier at the gas–solid interface the coordinate dependence of $C(x,t)$ is not as steep as in the case of a constant source. The concentration profiles observed in the experiment appeared to be even less steep. The reason could be the use of polycrystalline samples, since for crystallites whose z axis is normal or almost normal to the sample's surface the ^{18}O isotope concentration changes little with depth.

Now let us examine the behavior of $C(x,t)$ when the sample was heated in an atmosphere of ^{18}O at a constant rate α, or $T=T_0(1+\alpha\tau)$. This regime is the limit of isochronous annealing. The most interesting situation that takes into account the experimental data is that in which ^{18}O atoms consecutively occupy oxygen positions of various types. Here the maximum rate of processes in a given stage occurs in the absence of noticeable variations in the occupation of other layers where isotopic exchange has either almost been completed or has not even started. In this given approximation

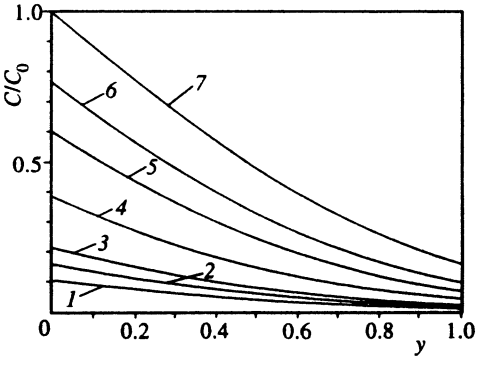

FIG. 7. Curves representing the calculated concentration profiles for the ^{18}O atoms in the $CuO_{1-\delta}$ plane in the presence of a barrier at the gas–solid interface. Curves *1–6* correspond to $\eta=0.01$, with $\tau/\tau_0=100$ (curve *1*), 250 (curve *2*), 500 (curve *3*), 2500 (curve *4*), 12 500 (curve *5*), and 50 000 (curve *6*). Curve *7* corresponds to the constant-source approximation: $C/C_0=\operatorname{erfc} y$.

Eqs. (1) yield the following equations for two consecutive stages in isotopic exchange:

$$\frac{\partial C^{(i)}}{\partial \tau} = \nu^{(i)} \exp\left\{ -\frac{E^{()}}{k_{\,B} T_0 (1+\alpha\tau)} \right\} \times (2C_{eq}^{(i-1)} - C^{(i)}), \quad i = 2,3, \tag{8}$$

where $\nu^{(2)}$ and $\nu^{(3)}$ are the pre-exponential factors in the rates of hopping of oxygen atoms between the $CuO_{1-\delta}$ and BaO planes and between the BaO and CuO_2 planes, $E^{(2)}$ and $E^{(3)}$ are the corresponding activation energies, k_B is the Boltzmann constant, and $C_{eq}^{(i)}$ are the equilibrium values of the oxygen concentration in the $YBa_2Cu_3O_{7-\delta}$ planes: $C_{eq}^{(1)} \simeq 1$ and $C_{eq}^{(2)} \simeq 2$. After substituting the solutions to Eqs. (8) into the expressions for $\partial C^{(i)}/\partial\tau$ with $i = 2,3$ we get

$$\frac{\partial C^{(i)}}{\partial \tau} 2C_{eq}^{(i)} = 2C_{eq}^{(i-1)} \nu^{(i)} \exp\left\{ -\frac{E^{(i)}}{k_{rmB} T_0 (1+\alpha\tau)} - m - \nu^{(i)} \int_0^{\tau} \exp\left(-\frac{E^{(i)}}{k_B T_0 (1+\alpha t)} \right) dt \right\}. \tag{9}$$

We see that peaks related to isotopic exchange can be present only if the following relationship linking the parameters holds true:

$$\nu^{(i)} \exp\left\{ -\frac{E^{(i)}}{k_{\,B} T_0} \right\} < \frac{\alpha E^{(i)}}{k_B T_0}, \quad i = 2,3.$$

The corresponding values of the times $\tau_0^{(i)}$ at which the $\partial C^{(i)}/\partial\tau$ assume their extremal values are given for $\alpha\tau \ll 1$ by

$$\tau_0^{(i)} = \frac{1}{\alpha}\left[\frac{E^{(i)}}{k_{\,B} T_0} + \ln \frac{\alpha E^{(i)}}{\nu^{(i)} k_{\,B} T_0} \right] \frac{1}{E^{(i)}/k_B T_0 + 2}. \tag{10}$$

Clearly, only continuous sets of values of $E^{(i)}$ and $\nu^{(i)}$ can agree with the experimental data, that is, $E^{(i)}$ must be a continuous function of $\nu^{(i)}$. Equations (9) and (10) make possible a rough estimate of the activation energies of the individual annealing stages proceeding only from the values of temperature at which there are peaks on the $\partial C/\partial T$ vs T curves. The reason is that fairly large variations in the rate factor $\nu^{(i)}$ cause the activation-energy to vary little: an increase in $\nu^{(i)}$ by a factor of ten lowers the activation energy $E^{(i)}$ by 0.1–0.15 eV.

3.2. A mathematical model for processes of isotopic exchange in $YBa_2Cu_3O_{7-\delta}$

The model used in numerical calculations incorporates the system of differential equations (1) and a set of boundary conditions of the form (2) for each of the $CuO_{1-\delta}$, BaO, and CuO_2 planes:

$$\frac{\partial C^{(1)}(0,t)}{\partial t} = \frac{\partial C^{(1)}(b,t)}{\partial t} = -\frac{2\mu}{1-\delta} C^{(1)}(0,t) + \mu C^{(2)}(0,t) + D_{xx}^{(2)} \frac{\partial C^{(1)}(0,t)}{\partial x} + \eta^{(1)}[1-\delta - C^{(1)}(0,t)],$$

$$\frac{\partial C^{(2)}(0,t)}{\partial t} = \frac{\partial C^{(2)}(b,t)}{\partial t} = \frac{2\mu}{1-\delta} C^{(1)}(0,t) - \mu C^{(2)}(0,t) + D_{xx}^{(1)} \frac{\partial C^{(2)}(0,t)}{\partial x} + \kappa C^{(3)}(0,t) + \eta^{(2)}[2 - C^{(2)}(0,t)], \tag{11}$$

$$\frac{\partial C^{(3)}(0,t)}{\partial t} = \frac{\partial C^{(3)}(b,t)}{\partial t} = \kappa[2C^{(2)}(0,t) - C^{(3)}(0,t)] + D_{xx}^{(3)} \frac{\partial C^{(3)}(0,t)}{\partial x} + \eta^{(3)}[4 - C^{(3)}(0,t)],$$

where the parameters $\eta^{(i)}$ characterize the rate of isotopic ith plane and the gaseous phase. It is clear that the number of diffusion parameters remains fairly high notwithstanding the artificial restriction on the number of subsystems in the oxygen sublattice. These parameters can be divided into three groups. The first characterizes the diffusion mobility of the oxygen atoms inside each crystallographic plane. The parameters belonging to this group are labeled by the subscript "b," including the pre-exponential factors for the hopping rates, $\nu_d^{(i)}$, and the activation energies $E_d^{(i)}$. The second group of parameters, $\nu_b^{(i)}$ and $E_b^{(i)}$, labeled by the letter "b," characterize the isotopic exchange on the boundary between the ith plane and the gaseous phase. The parameters of isotopic exchange between $CuO_{1-\delta}$ and BaO planes ($\nu^{(2)}$ and $E^{(2)}$) and between BaO and CuO_2 planes ($\nu^{(3)}$ and $E^{(3)}$) were introduced earlier. An additional variable parameter is the average crystallite size b.

Using the mathematical model, we were able to show that a set of parameters can be chosen that provide a satisfactory description of the experimental data of the kind shown in Figs. 1–5. The calculated characteristic curves representing the temperature dependence of $\partial C/\partial T$ (Fig. 8) correspond to depths near the sample surface, that is, to the experimental conditions. In view of the large number of parameters, certain restrictions originating from the experimental results were imposed on the range of their variation. For instance, the weak dependence of the concentration profile on the depth x suggests that there is a sizable barrier of height $E_b^{(1)}$ at the boundary between a $CuO_{1-\delta}$ layer and the gaseous phase. Calculations show that in these conditions variations in the parameters $\nu_d^{(1)}$ and $E_d^{(1)}$ have only a slight effect on the temperature dependence of $\partial C/\partial T$ at temperatures near the first peak. On the other hand, variations in $\nu_b^{(1)}$ and $E_b^{(1)}$ and the grain size b have a strong effect. The range of $E_d^{(1)}$ from 0.9 to 1.1 eV at $\nu_d^{(1)} = 10^{12}$ Hz corresponds to the obtained experimental data. As the grain size increases from 2 to 8 μm (with all the other parameters remaining constant), the first peak shifts by approximately 50 °C toward higher temperatures. The average grain size can quite easily be determined independently. Then an approximate estimate of the height of the energy barrier at the sample's surface can be done using only the temperature at which the $\partial C/\partial T$ vs T curve has its first peak. This possibility stems from the fact that the activation energy $E_b^{(1)}$ changes only slightly with $\nu_b^{(1)}$ the value of $E_b^{(1)}$ diminishes by 0.1–0.15 eV when $\nu_b^{(1)}$ increases by a factor of ten. Thus,

the temperature dependence of $\partial C/\partial T$ in the temperature range of the first peak is determined primarily by processes taking place at the gas–solid interface. In view of this, the value of the activation energy for the first peak listed in Table I has no definite physical meaning, and the optimum value $E_b^{(1)}$ found as a result of modeling must be considered an estimate of the height of the barrier that the oxygen atoms pass through when "traveling" from the gaseous phase to their positions in a $CuO_{1-\delta}$ plane.

On the basis of an analysis of the second and subsequent peaks we can identify the mechanism by which ^{18}O atoms substitute for ^{16}O atoms occupying positions in BaO and CuO_2 planes. In the diffusion mechanism the arrival of ^{18}O atoms in BaO and CuO_2 planes is limited by the energy barrier at the gas–solid interface, with the arriving ^{18}O atoms diffusing in the respective planes. In the alternative variant, related to the drain mechanism, ^{18}O occupy the positions in BaO and CuO_2 planes because of isotopic exchange between planes inside the crystal. Calculations show that when the diffusion mechanism is predominant, the shape of the $\partial C/\partial T$ vs T curve displays no distinct annealing peaks. In this sense the experimental data of Fig. 1 contradict the diffusion mechanism and agree only with the drain mechanism of isotopic exchange (Fig. 8). The minimum between the second and first peaks becomes deeper if we allow for the presence of two oxygen subsystems in a CuO_2 plane.

Thus, there is certainly a difference between the mechanisms of isotopic exchange for positions in a $CuO_{1-\delta}$ plane and all those for other positions. Accordingly, the values of E_n for the second, third, and fourth peaks listed in Table I appear to be physically meaningful.

This technique does not allow the activation energy to be determined for the migration of tracer oxygen atoms from one CuO_2 plane to another. Such information can be extracted by comparing the E_n values with the activation energy of diffusion along the z axis, provided that this energy exceeds E_3, since otherwise the value of the activation energy $E_3 = 2.26$ eV, listed in Table I, limits the diffusion along the z axis. Unfortunately, we do not know of any such data for $YBa_2Cu_3O_{7-\delta}$. Note that the value E_3 proves to be close to the values of the activation energy of diffusion of oxygen along the z axis in bismuth high-T_c superconductors: 2.11 eV for $Bi_2Sr_2CuO_x$ (Ref. 3) and 2.20 eV for $Bi_2Sr_2CaCu_2O_x$ (Ref. 4).

4. CONCLUSION

Our study has demonstrated the possibility of independently determining an entire set of diffusion parameters, which means that conditions can arise such that diffusion in the $YBa_2Cu_3O_{7-\delta}$ crystal cannot be considered in the continuous-medium approximation. Hence there is no unique correspondence between the diffusion tensor of the tracer oxygen atoms, D_{ik}, and the concentration profiles $C(x,\tau)$. The behavior of the latter depends sensitively on the hopping rates of the atoms. These rates have practically no effect on the components of the tensor D_{ik} in conditions corresponding to the continuous-medium approximation. Similar results can be obtained for the diffusion of tracer oxygen atoms in other high-T_c superconductors with a quasi-planar structure and an anomalously high anisotropy of the diffusion properties. This suggests assigning a separate class of diffusion systems to these objects. Within this class the diffusion processes with ordinary temperature-temporal annealing parameters are not described by the Fick equation. Naturally, this requires a critical analysis of the experimental data on oxygen diffusion obtained through the use of a solution of the second Fick equation. As an alternative, we suggest in this paper a system of equations (1) that, in a certain sense, are similar to the Fisher equations for diffusion in polycrystals. Note, however, that the scales on which these phenomena operate are essentially different: in a single crystal only some atomic planes participate in the drain processes, while in polycrystals the drain of atoms from grain boundaries encompasses a region whose size amounts to many interatomic distances.

As a result of this investigation we have obtained a much fuller set of values of the energy barriers encountered in the migration of oxygen atoms than was previously possible. Some energy and rate parameters require further refinement. One reason for this is that the experiments involved a polycrystal, whereas the theory was built for a single crystal of $YBa_2Cu_3O_{7-\delta}$. Since ^{18}O atoms replace ^{16}O atoms in positions in BaO and CuO_2 planes via the drain mechanism, the respective corrections should refer, primarily, to the first stage of isotopic exchange. The next step in studying the diffusion mechanism must be a study of the correlation effects and temperature dependence of the vacancy concentration in various positions of the oxygen sublattice of the

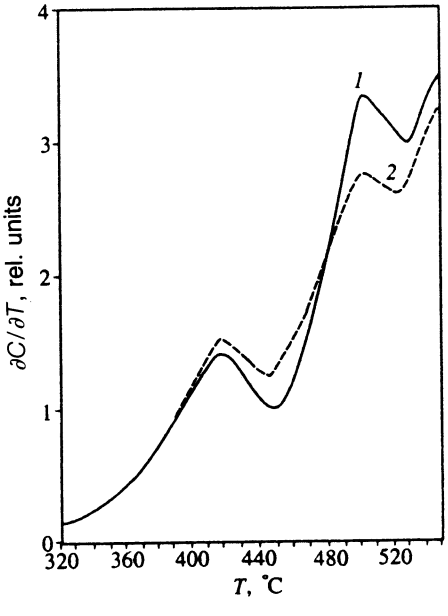

FIG. 8. Curves representing the calculated temperature dependence of $\partial C/\partial T$ for the drain mechanism of isotopic exchange in the second and third annealing stages. The following parameters were used: $\alpha^{-1} \simeq 4.3\times 10^5$ s, $b = 6.5$ μm, $E_b^{(1)} \simeq 1.7$ eV, $E_d^{(1)} \simeq 1.1$ eV, $E^{(3)} \simeq 2.3$ eV, $\nu_b^{(1)} = \nu_d^{(1)} = 10^{12}$ Hz, $\nu_b^{(2)} = \nu_d^{(2)} = 0$, and $\nu^{(3)} = 2\times 10^9$ Hz; curve *1* corresponds to $E^{(2)} = 2.15$ eV and $\nu^{(2)} = 5\times 10^9$ Hz, and curve *2* to $E^{(2)} = 1.65$ eV and $\nu^{(2)} = 2.5\times 10^6$ Hz. T, °C

$YBa_2Cu_3O_{7-\delta}$ crystal. Two points must be stressed here. First, a large difference in activation energy values (about 0.7 eV) was reported when ^{18}O took up almost identical types of positions in a CuO_2 plane. In view of this, it is quite possible that the diffusion of oxygen atoms in the direction of the z axis manifests strong correlation effects and/or that not only thermally equilibrium vacancies but structural vacancies, too, are responsible for the migration of oxygen atoms along this axis.

The second point has to do with the pre-exponential factors in the hopping rates. The time curves $c(\tau)$ in Figs. 2–5 are described by the equation

$$c(\tau)=\Delta c_n(1-\exp\{-\Gamma_n\tau\}),$$

where for the established mechanism of substitution of ^{18}O atoms for ^{16}O atoms in positions in BaO and CuO_2 planes the coefficients Γ_n represent hopping rates. Since the activation energies for Γ_n were obtained independently, it was possible to determine the pre-exponential factors for the hopping rates ν_n (see Table I). The difference in the values of ν_n proved so great that it was impossible to explain its origin in the vibration frequencies and activation entropies. Thus, there is additional cause to believe that there are strong correlation effects and that structural vacancies participate in diffusion along the z axis.

In conclusion we note a consequence of our study that is of practical importance. The method of isochronous annealing can ensure the substitution of only the ^{18}O or ^{16}O isotope for almost any kind of equilibrium positions. For instance, for ^{18}O atoms to occupy the O4 positions in the BaO plane, we must first carry out annealing in an ^{18}O atmosphere, which puts ^{18}O atoms into the O1, O5, and O4 positions, followed by annealing in an ^{16}O atmosphere, to substitute for the O1 and O5 positions. Samples with such properties are useful in studying the nature of superconductivity and a number of physical properties of the systems in question.

This work was supported by the Scientific Council on High-T_c Superconductivity and carried out as part of Project No. 90 040 of the National Program for Superconductivity Studies, and by the International Science Foundation (Project Ph 2-5747, ISF).

[1] A. Damask and G. Dienes, *Point Defects in Metals*, New York, 1969.
[2] S. J. Rothman, J. L. Routbort, J.-Z. Liu *et al.*, Defect and Diffusion Forum **75**, 57 (1991).
[3] M. Runde, J. L. Routbort, J. N. Mundy *et al.*, Phys. Rev. B **46**, 3142 (1992).
[4] M. Runde, J. L. Routbort, and S. J. Rothman, Phys. Rev. B **45**, 7375 (1992).
[5] S. Tsukui, Y. Yamamoto, M. Adachi *et al.*, Physica C **185–189**, 929 (1991).
[6] K. Kishio, J. Shimoyama, T. Hasegawa *et al.*, Jpn. J. Appl. Phys. **26**, L1228 (1987).
[7] V. B. Vykhodets, T. E. Kurennykh, A. A. Fotiev *et al.*, Pis'ma Zh. Eksp. Teor. Fiz. **58**, 421 (1993) [JETP Lett. **58**, 431 (1993)].
[8] V. B. Vykhodets, T. E. Kurennykh, A. Ya. Fishman *et al.*, Dokl. Akad. Nauk **330**, 207 (1993).
[9] S. Z. Bokshteĭn, S. S. Ginzburg, S. T. Kishkin *et al.*, *Autoradiography of Interfaces and the Structural Stability of Alloys*, Metallurgiya, Moscow, 1978 [in Russian].

Translated by Eugene Yankovsky

This article was translated in Russia. It is reproduced here the way it was submitted by the translator, except for stylistic changes by the Translation Editor.